Polymer Bulletin (2020) 77:1847–1868
https://doi.org/10.1007/s00289-019-02836-6

ORIGINAL PAPER

Preparation and flocculation properties of biodegradable konjac glucomannan-grafted poly(trimethyl allyl ammonium chloride)

Dating Tian[1,2] · Yuchi Zhou[1] · Kai An[1] · Huiting Kang[1]

Received: 28 March 2019 / Revised: 6 June 2019 / Accepted: 9 June 2019 / Published online: 12 June 2019

Abstract

Preparation of konjac glucomannan-grafted poly(trimethyl allyl ammonium chloride) (KGM-*g*-PTMAAC) was carried out using KGM as polysaccharide matrix and TMAAC as cationic comonomer to develop biodegradable flocculants. The structure of KGM-*g*-PTMAAC was characterized by FTIR, ^{13}C solid-state NMR, elemental analysis (EA) and SEM. Thermal properties of KGM-*g*-PTMAAC were studied by thermal gravimetric (TG) analysis. In addition, flocculation properties of KGM-*g*-PTMAAC were investigated in a kaolin suspension. The results of the FTIR, NMR, and EA showed that the cationic moiety containing quaternary ammonium has been introduced in the backbone of KGM. SEM images indicated that the surface of KGM-*g*-PTMAAC was rougher than that of KGM. TG results indicated that the thermal stability of KGM-*g*-PTMAAC was different to that of KGM. The obtained products had a good biodegradable performance. Moreover, the results of the flocculation test showed that KGM-*g*-PTMAAC could be potentially used as a good flocculating agent.

Keywords Graft copolymerization · Konjac glucomannan · Flocculant · Biodegradable · Trimethyl allyl ammonium chloride

Introduction

With the continuous advancement of industrialization, water resources problems in various countries around the world have become increasingly serious, mainly due to the scarcity and the increasing pollution situation of water resources. In particular,

✉ Dating Tian
tiandating@163.com

[1] School of Chemical and Environmental Engineering, Hubei Minzu University, Enshi 445000, People's Republic of China

[2] Key Laboratory of Biologic Resources Protection and Utilization of Hubei Province, Hubei Minzu University, Enshi 445000, People's Republic of China

industrial sewage and domestic sewage become the main source of water pollution. Seeking low-cost and high-efficiency water pollution treatment is one of the problems that we urgently need to solve, and also an inevitable requirement for sustainable development. At present, there are various water treatment methods [1], such as flocculation [2], biochemical treatment [3], ion exchange [4], adsorption [5], chemical oxidation [6], microbial method [7] and so on. However, the lowest cost and most widely used treatment method is still flocculation method. The flocculation method is as follows: adding specific chemical substances (i.e., flocculants) to the wastewater to be treated, and under the action of chemistry, physics and physical chemistry, the fine substances in the original wastewater which are difficult to be settled and filtered are aggregated to form large flocs, and settled down, and then can be simply separated from water.

The commonly used flocculants can be divided into three categories: inorganic flocculants, synthetic polymer flocculants, and natural polymer flocculants. Among them, inorganic flocculants are mainly represented by aluminum salts, iron salts and magnesium salts, which are widely used for printing and dyeing wastewater treatment. However, the defect of inorganic flocculants is that the dosage is high, and the residual amount in the water is high, which inevitably causes secondary pollution of water. Although synthetic polymer flocculants such as polyacrylamide and polyacrylic acid have good flocculating performance, their applications are limited because they are difficult to be degraded and have certain toxicity due to the use of synthetic monomers.

With the enhancement of people's awareness of environmental protection and sustainable development, flocculants based on natural polymers have been attracting more attention due to the properties of pollution-free, biodegradability, low cost, non-toxicity, and abundance. Recently, a large number of natural flocculants have been developed using natural polymers such as starch [8], cellulose [9], chitosan [10], guar gum [11] and so on. Moreover, cationic flocculants have attracted more and more attention because the surface of pollutant particles in modern industrial and domestic drainage is usually negatively charged [12, 13]. Therefore, a large number of cationic natural polymer flocculants have been developed [11, 14–16]. Relatively, there are not many researches on the cationic KGM-based flocculant.

Konjac Glucomannan (KGM) is a kind of natural polysaccharide extracted from *Konjac* tuber, which is composed of D-glucose and D-mannose linked by β-1,4-glycosidic bond in a molar ratio of about 1:1.6 [17]. Because of its hydrophilic, edible, gelatinous and degradable properties, KGM has been widely used in food, medicine, chemical industry, agriculture, bioengineering and other fields [18–20]. Cationization of KGM is one of the important means of chemical medication for KGM. Lei et al. [21] reported the preparation and antimicrobial activity of KGM modified with a quaternary ammonium compound. Yu et al. [22] used KGM to react with 3-chloro-2-hydroxypropyltrimethylammonium chloride (CHPTAC) in the presence of sodium hydroxide to prepare a quaternary ammonium derivative of KGM and studied its antimicrobial activity. Recently, Gao et al. [23] reported a homogenous method of synthesized cationic KGM in NaOH/urea by reacting KGM with 3-chloro-2-hydroxypropyltrimethylammonium chloride (CHPTAC). Using 2, 3-epoxypropyl trimethyl ammonium chloride (EPTMAC) as cationization reagent,

our group [24] recently synthesized quaternary ammonium cationic KGM by the dry method and found the obtained product was a kind of flocculants. Recently, Zhang et al. [25] prepared a cationic polymer by grafting KGM with poly-(2-methacryloyloxyethyl)trimethyl ammonium (PDMC) and evaluated their flocculation properties; however, they did not investigate the biodegradability of the products. In general, most of cationic flocculants based on KGM mentioned above are realized on the etherification. Etherification may inevitably involve more or less side reactions and/or use a lot of organic solvents. Obviously, grafting copolymerization can effectively avoid these drawbacks. Nevertheless, there are not many reports on the preparation of cationic flocculants by grafting modification of KGM.

Although the closed vessel method for grafting copolymerization is a conventional method, it has many advantages such as relatively simple operation and no special equipment, so it is still used by many researchers [26–28]. In addition, according to the literature [26, 29], if ceric (IV) ammonium nitrate is applied as an initiator in the grafting modification of polysaccharides, the absence of free radical initiators in the reactive medium can limit the formation of homopolymer, and at the same time, the reaction can be easily carried out at lower temperature in aqueous medium. As far as the cost and the benefit are concerned, the closed vessel method is also used to prepare the grafting copolymer of KGM.

Therefore, in this work, a novel cationic flocculant of biodegradable KGM grafted poly(trimethyl allyl ammonium chloride) was prepared in aqueous solution using trimethyl allyl ammonium chloride (TMAAC) as cationic comonomer and cerium ammonium nitrate (CAN) as initiator. And flocculation properties of KGM-*g*-PTMAAC were evaluated in kaolin suspensions. Moreover, the biodegradable behavior of the resultant flocculant was also investigated.

Materials and methods

Materials

Konjac glucomannan (KGM), supplied by Hubei Enshi Hongye Konjac Co., Ltd., was refined with ethanol before use and dried *in vacuum* to constant weight. Trimethyl allyl ammonium chloride (TMAAC) was purchased from Jintan Southwest Chemical Research Institute. Other reagents were analytically pure without any treatment before use.

Synthesis of KGM-*g*-TMAAC

The synthesis process was presented in line with Scheme 1 [21, 30]. Namely, a proper amount of deionized water (200 mL) was added to a tri-necked bottle with a constant pressure titration funnel, and a certain amount of KGM and CAN were added in the stirring state. A certain amount of TMAAC was dissolved in deionized water to form a 25% solution (4–36 mL) and then was put into a constant pressure titration funnel. The temperature of the reaction system was raised to a certain temperature under the

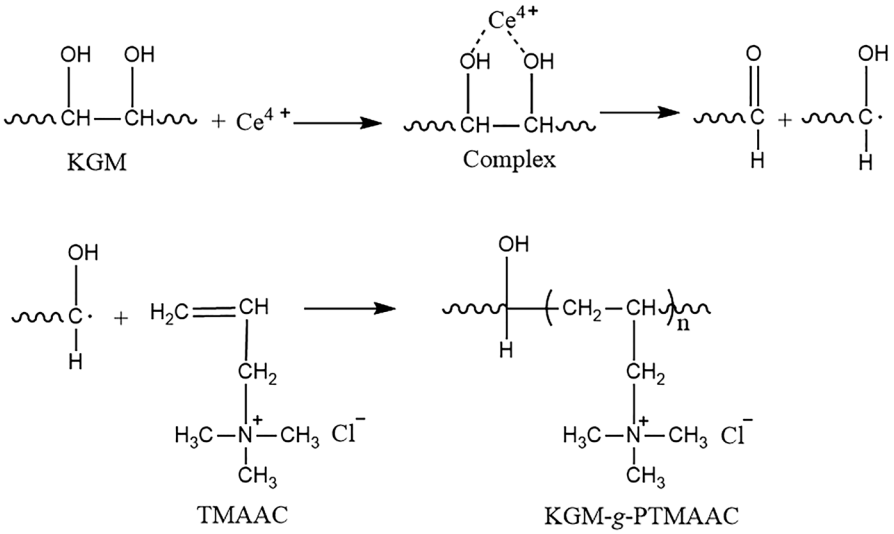

Scheme 1 Possible reaction of KGM with TMA AC

protection of nitrogen, and TMAAC solution was added after 10 min to carry out the grafting copolymerization.

Moreover, the purification of the products could be described as follows [15, 31]. After the reaction was completed, the products were precipitated using an excess of anhydrous ethanol, washed with anhydrous ethanol 5 times, separated by filtration, and then extracted using ethanol/water (4/1, v/v) as solvent in a Soxhlet apparatus for 24 h to remove all unreacted monomer and homopolymer [30, 32, 33]. Afterward, the purified products were dried *in vacuum* at 35 °C. At the end, they were crushed and weighed in turn.

The grafting yield (GY) was calculated from the following formula [31, 34].

$$\mathrm{GY}(\%) = \frac{W_1 - W_0}{W_0} \times 100 \tag{1}$$

where GY, W_1 and W_0 represented the grafting yield of graft copolymers, the weight of obtained products (KGM-*g*-PTMAAC) and the weight of KGM, respectively.

Moreover, using initiator amount, reaction temperature, reaction time and monomer amount as experimental factors, respectively, an orthogonal experiment with four factors and three levels, i.e., L9(3^4) matrix was carried out to clarify the interaction between the parameters. The design of orthogonal experiment is listed in Table 1.

FTIR

FTIR spectra of graft polymers were carried out using a KBr pellet method with Avatar 370 Fourier transform infrared spectrometer of Thermoelectric Co., LTD, USA.

Table 1 Factors and levels of orthogonal experimental of L9(3^4)

Levels	Factors			
	A	B	C	D
	CAN/(KGM + TMAAC) (wt%)	T (°C)	t (h)	m_{TMAAC}/m_{KGM}
Level 1	0.5	60	4.0	7.0
Level 2	0.9	70	3.0	3.0
Level 3	0.7	80	5.0	5.0

^{13}C CP/MAS NMR

^{13}C CP/MAS NMR experiment was performed on Bruker AVANCE III 600 spectrometer at a resonance frequency of 150.9 MHz. ^{13}C CP/MAS experiments were performed on a 4 mm probe with a contact time of 3 ms, a recycle delay of 4 s, and a sample spinning rate of 12 kHz. The chemical shifts of ^{13}C were externally referenced to TMS.

Elemental analysis

The elemental analysis of samples was taken by PerkinElmer 2400 Series II elemental analyzer. The contents of C, H and N were determined.

Zeta potential

A sample solution (4 mg/L) was thoroughly stirred, and then the Zeta potential was measured using a Nano-ZS Zetasizer (Malvern Instruments, UK). The pH values were adjusted by 0.01 mol/L HCl or 0.01 mol/L NaOH aqueous solution.

TG analysis

The thermal stability of graft polymers was analyzed after fully dried and accurately weighed. Under N_2, TG analysis was carried out with TG/DTA6300 made by Japanese Seiko, with heating rate of 20 °C/min and scanning temperature range of 30–600 °C.

SEM

The morphology of samples dried *in vacuum* was observed using the JSM-6510LV scanning electron microscope manufactured by the Japan Electronics Corporation.

Flocculation experiment

The flocculation performance of KGM-*g*-PTMAAC was carried out using standard Jar Test method [35, 36]. Firstly, 200 mL of 1.0 wt% kaolin suspension was used to simulate waste water. Then, a certain amount of graft copolymers was added to the kaolin suspension and was stirred at 25 rpm for 2 min. The turbidity of the supernatant was measured by WGZ-200 photoelectric turbidity meter (Shanghai Precision Instrument Company, China). The turbidity removal rate (Tr, %) was calculated as follows [35, 36].

$$\mathrm{Tr}(\%) = \frac{T_0 - T_1}{T_0} \times 100 \tag{2}$$

where T_0 and T_1 represents the turbidity of kaolin suspension before treatment (nephelometric turbidity units, NTU) and the turbidity of kaolin suspension after treatment (NTU), respectively.

Biodegradation studies

The biodegradation performance of KGM-g-PTMAAC was tested using soil extract [37]. 100 g of fresh soils was added into 200 mL of deionized water and vigorously stirred using a stirrer for 20 min, and then centrifuged with a high-speed centrifuge at 6000 r/min for 15 min. Then fine particles and impurities in the soil supernatant were removed by filtration, and the filtrate was diluted to 200 mL with deionized water for biodegradation experiment.

0.2 g of KGM-g-PTMAAC was added to the above 200 ml of the soil extract and was incubated at 37 °C in an incubator. After having been degraded for every interval, these samples were taken out and washed with 100 mL absolute ethanol to remove the impurities on the surface, then dried and weighed, respectively.

The degradation ratio (DR) could be determined by measuring the weight loss of sample, which was calculated by the following formula [38]:

$$\mathrm{DR}(\%) = \frac{W_0 - W_i}{W_0} \times 100$$

where DR is the degradation rate of the sample, W_i is the residual weight of the sample after i d, and W_0 is the weight of the original sample.

Results and discussion

Synthesis of the graft copolymer

Effect of time on graft copolymerization

In this grafting copolymerization, Ce^{4+} was selected as initiator, which has some following advantages [30]. For example, there were few free initiators in the reactive medium, limiting the formation of homopolymers, and moreover, the reaction was easy to carry out in aqueous solution. Nevertheless, some homopolymers would inevitably be formed during graft copolymerization. However, both these homopolymers and unreacted monomers could be removed by Soxhlet extraction method [25, 33]. When the weight ratio of TMAAC/KGM was 5:1, the weight ratio of CAN/(KGM + TMAAC) was 0.7%, and the reaction temperature was 70 °C; the influence of reaction time on the grafting yield is shown in Fig. 1. As shown in Fig. 1, the grafting yield increased with the extension of reaction time and reached a maximum value at 4 h, and then the values decreased after 4 h. This could be explained that there were a large number of active sites on KGM backbone in the early stage of reaction, and the grafting yield increased due to the rapid graft reaction. However, with the reaction proceeding, the grafting yield decreased. Many researchers reported similar results, and most of them believed that the reduction of the grafting yield with time might be interpreted as follows [39, 40]. On the one hand, the increased viscosity of the system retarded the diffusion of the monomers to reach the active sites on the KGM. On the other hand, the number of site available for grafting reduced due to the consumption of initiators. Moreover, another possible explanation was the fragmentation of KGM chain in the presence of Ce^{4+}. The obtained

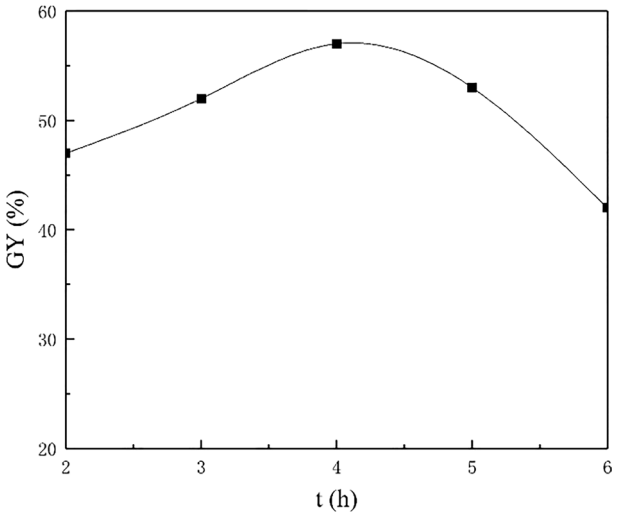

Fig. 1 Effect of reaction time on graft copolymerization (5:1 TMAAC/KGM, 0.7% CAM/(KGM + TMAAC), 70 °C)

low molecular KGM chains were not all precipitated in the ethanol–water mixture, which also results in a decrease in the measured grafting yield. The optimal reaction time was selected as 4 h.

Effect of weight ratio of TMAAC to KGM on graft copolymerization

Figure 2 shows the influence of weight ratio of TMAAC to KGM on the graft yield. It can be seen from Fig. 2 that when the weight ratio was less than 5:1, the grafting yield increased with the increase in the TMAAC/KGM ratio, and when the weight ratio was higher than 5:1, the grafting yield did not increase any more.

When the weight ratio was low, the probability of collision between TMAAC and KGM in the system was low, and TMAAC and KGM did not fully react. With the increase in TMAAC dosage, the probability of contacting between KGM active sites and TMAAC increased, then the graft yield increased. However, when too much TMAAC was added into the system, the homopolymerization of TMAAC was easy to occur, and the resulting homopolymers could not graft with KGM, thus reducing the grafting yield. Therefore, 5:1 of TMAAC to KGM was chosen as the appropriate dosage.

Effect of amount of initiator on graft copolymerization

Figure 3 shows the effect of amount of Ce^{4+} on the grafting yield in the case of other reaction parameters being fixed. When the weight ratio of CAM/(KGM + TMAAC) was lower than 0.7%, the grafting yield increased with the increase in the Ce^{4+} amount; however, when the weight ratio was higher than 0.7%, the grafting yield decreased. Because Ce^{4+} reacted with KGM to produce free radicals, and the

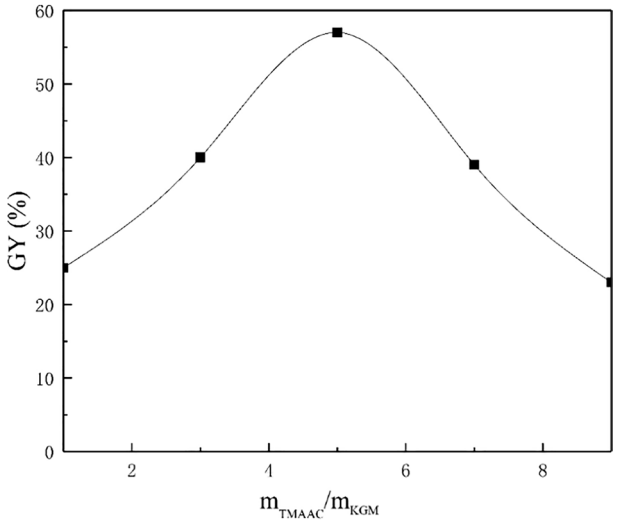

Fig. 2 Effect of weight ration of TMAAC to KGM on graft copolymerization (0.7% CAM/(KGM + TMAAC), 70 °C, 4 h)

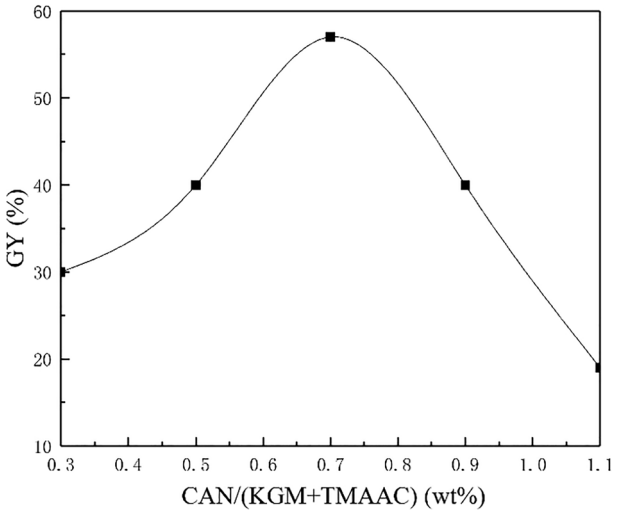

Fig. 3 Effect of amount of initiator on graft copolymerization (5:1 TMAAC/KGM, 70 °C, 4 h)

number of free radicals increased as the increase in the Ce^{4+} concentration, resulting in the increase in the grafting yield. However, when the Ce^{4+} concentration was high enough, free radicals probably transfer to initiators, that is, induced decomposition occurs, thus reducing the grafting yield.

Effect of temperature on graft copolymerization

Figure 4 shows the temperature on the graft copolymerization when other reaction parameters were fixed. It can be seen from Fig. 4 that the grafting yield increased with the increase in temperature when the temperature was lower than 70 °C, and then decreased with the increase in temperature when the temperature was higher than 70 °C.

When the reaction temperature was too low, the generation rate of the primary radicals was slow, and the probability of TMAAC contacting with the radical was relatively low, then the grafting reaction could not be fully carried out. As the reaction temperature increased, CAM could react with KGM to form more active sites, resulting in increased grafting yield. However, when the reaction temperature was higher than 70 °C, the reaction occurred too fast, causing some side reactions such as chain transfer and/or fracture of molecular chains, then the grafting yield decreased. In this system, the best reaction temperature was 70 °C.

Analysis of orthogonal experiments

In order to study the influence of multiple factors on the graft copolymerization of KGM with TMAAC, a four-factor and three-level orthogonal experiment, i.e., $L9(3^4)$ matrix was carried out using initiator amount (A), reaction temperature (B), reaction time (C) and monomer amount (D) as experimental factors, respectively.

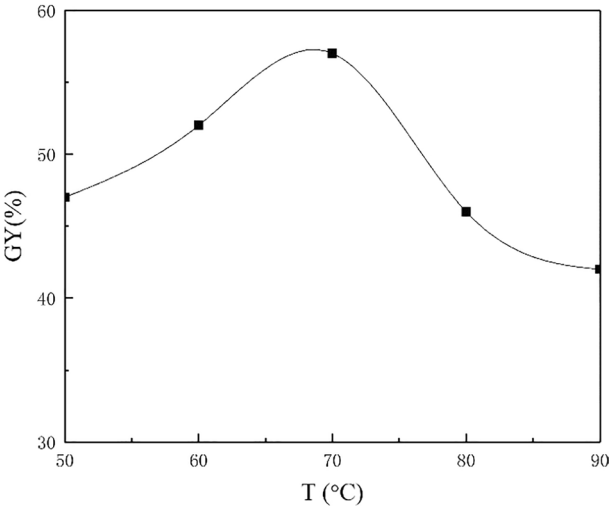

Fig. 4 Effect of temperature on the graft copolymerization (5:1 TMAAC/KGM, 0.7% CAM/(KGM + TMAAC), 4 h)

The design of orthogonal experiments is shown in Table 1. The orthogonal experiment of L9(3^4) matrix was conducted according to Table 1, and the result of orthogonal experiments was obtained, as shown in Table 2.

In Table 2, k_1, k_2 and k_3 represents the average grafting yield of the graft copolymer at each level of each factor, respectively. And Ri is the extreme difference of the average grafting yield at all levels under the same factor. Generally, the average value reflects the influence of different levels under the same factor on the experimental

Table 2 Results of orthogonal experiments

No.	Factors				GY (%)
	A	B	C	D	
1	A_1	B_1	C_1	D_1	45.05
2	A_1	B_2	C_2	D_2	48.00
3	A_1	B_3	C_3	D_3	44.12
4	A_2	B_1	C_2	D_3	46.06
5	A_2	B_2	C_3	D_1	49.00
6	A_2	B_3	C_1	D_2	49.20
7	A_3	B_1	C_3	D_2	49.98
8	A_3	B_2	C_1	D_3	57.30
9	A_3	B_3	C_2	D_1	52.00
k_1	45.72	47.03	50.52	48.68	
k_2	48.09	51.43	48.69	49.06	
k_3	53.09	48.44	47.70	49.16	
R_i	7.37	4.40	2.82	0.48	

results, and it determines the optimal level under that factor. The extreme difference reflects the magnitude of the influence of the level change of each factor on the experimental results. The high value of extreme difference indicates that the level change of this factor has strong impact on the experimental results. On the contrary, it has a weak impact on the experimental results.

Therefore, as shown in Table 2, the optimal combination of various factors was $A_3B_2C_1D_3$, namely the optimal process condition was 0.7% of initiator amount, 70 °C of reaction temperature, 4 h of reaction time and 5:1 of m_{TMAAC}/m_{KGM}, respectively, which was consistent with the previous experimental results. Moreover, according to the magnitude of extreme difference, the influencing order of each factor followed as A > B > C > D. In particular, it should be pointed out that in this work, the samples used for further structural characterization and performance testing were prepared under the optimal condition.

Characterization of the samples

FTIR of the graft copolymers

The infrared spectra of KGM (a) and KGM-*g*-PTMAAC (b) are shown in Fig. 5. As shown in Fig. 5a, the broad peak at 3390 cm^{-1} was attributed to the stretching vibration absorption of O–H in KGM, and the peak at 1644 cm^{-1} was caused by the first overtone of O–H bending vibration. The peak at 1727 cm^{-1} was attributed to the C=O stretching vibration absorption of acetyl groups in KGM, and two peaks at 1065 and 1025 cm^{-1} were due to the C–O–C stretching vibration absorption. Comparing the infrared spectra of KGM and that of KGM-*g*-PTMAAC, it could be found from Fig. 5b that besides the characteristic absorption peaks of KGM, there were the bending vibration absorption peak of methylene bonded with N^+ at 1430 cm^{-1}, the in-plane asymmetric bending

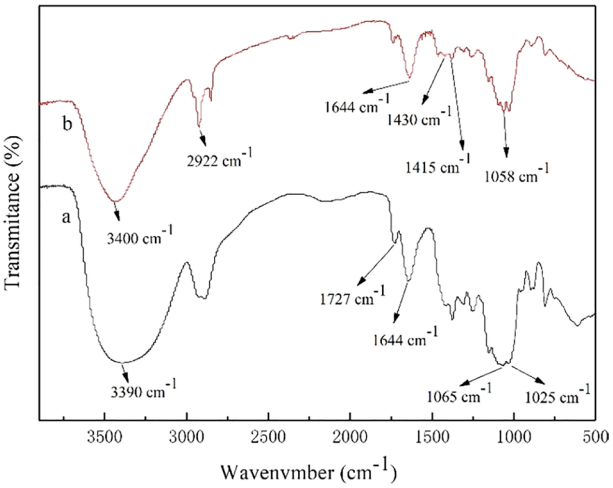

Fig. 5 FTIR spectra of KGM (a) and KGM-*g*-PTMAAC (b)

vibration absorption peak of methyl bonded with N^+ appeared at 1415 cm^{-1}, and the C–C stretching vibration absorption peak of ammonium salt at 1058 cm^{-1}. Moreover, the peak at 2922 cm^{-1} was attributed to C–H stretching of methane in the TMAAC. All above indicated that TMAAC were successfully grafted onto the main chain of KGM.

^{13}C solid-state NMR spectroscopy

The ^{13}C solid-state NMR spectra of KGM (a) and KGM-*g*-PTMAAC (b) are shown in Fig. 6. The assignment of ^{13}C NMR peaks of KGM was suggested on the basis of previous solid-state NMR work on KGM [17, 41–43]. The peak at 102.42 ppm was the characteristic anomeric signal due to C-1 resonance of sugar ring and that at 61.60 ppm was attributed to the resonance of pendant methylene carbon of C-6. The peaks from 81.30 to 68.45 ppm overlapped to some extent due to the complex nature of the spectra of polysaccharides; however, they corresponded to the remaining carbon atoms in the KGM backbone, which could be assigned as C-4 (81.30 ppm), C-5 (75.26 ppm), C-3 (73.10 ppm), and C-2 (68.45 ppm), respectively. Comparing the ^{13}C NMR spectra of KGM and that of KGM-*g*-PTMAAC, it could be found from Fig. 6b that besides the characteristic peaks of KGM, there appeared some new peaks in the latter. The sharp new peak at 53.62 ppm was due to the resonance of *N*-methyl carbon of quaternary ammonium salt [22, 44]. The peak at 70.00 ppm was attributed to the resonance of propyl carbon directly connected to N^+. Furthermore, the two peaks appearing around 130 ppm were the resonance of two carbonyl carbons at the sugar ring. In all, the ^{13}C solid-state NMR spectroscopy also confirmed the structure of the graft copolymer.

Elemental analysis and Zeta potential of sample

The results of elemental analysis of KGM and KGM-*g*-PTMAAC (typical sample) are listed in Table 3. As shown in Table 3, the amount of N in KGM was very low, which might be related to the presence of trace quantities of proteins in the commercial polysaccharides. However, the content of N in the graft copolymer was significantly higher, which indicated that the presence of graft chain of PTMAAC. According to the count of N, the weight ratio of PTMAAC to KGM was determined as 0.57:1, which was consistent with the grafting yield of the KGM-g-PTMAAC.

In addition, Fig. 7 presents the influence of pH on the Zeta potential of the KGM-*g*-PTMAAC solution. As shown in Fig. 7, the solution of the graft copolymer had a positive Zeta potential at all measured pH range from 2.0 to 12.0. This phenomenon was attributed to the introduction of cationic quaternary ammonium salt groups on the KGM. Of course, both the elemental analysis results and the Zeta potential results further supported the success of the graft copolymerization.

Morphology of samples

Figure 8 shows an SEM image of KGM and that of KGM-*g*-PTMAAC, respectively. Macroscopically, KGM and KGM-g-PTMAAC were spherical particles. However, on the micro-level, they were irregular-shaped with different morphologies. The

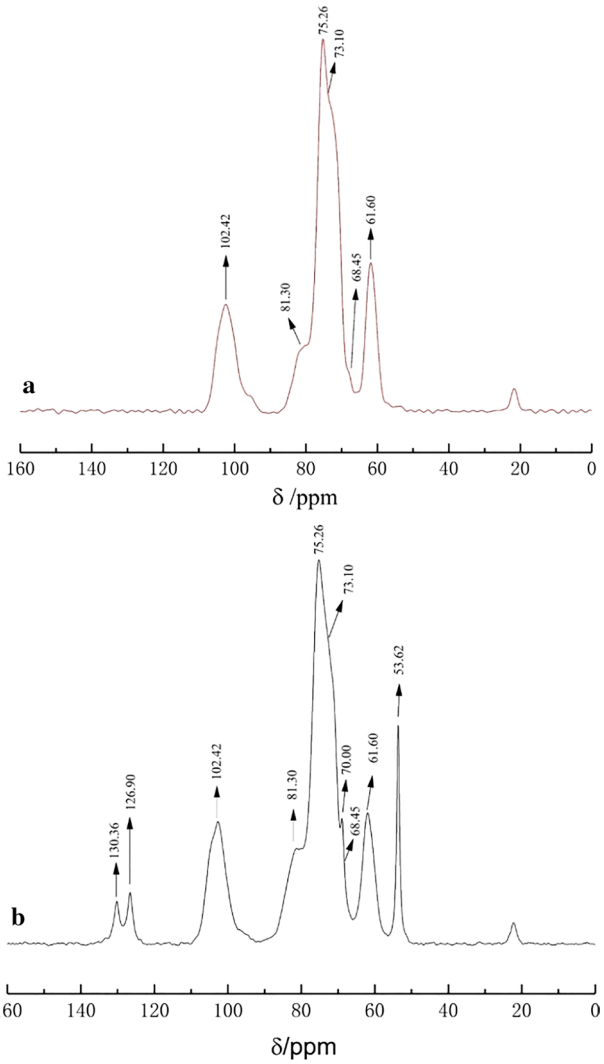

Fig. 6 ^{13}C solid-state NMR spectra of KGM (**a**) and KGM-*g*-PTMAAC (**b**)

Table 3 Results of element analysis of typical samples

Sample	C (%)	H (%)	N (%)
KGM	44.12	6.16	0.10
KGM-*g*-PTMAAC	47.20	7.65	3.74

SEM image of KGM indicated that it had a relatively smooth surface, and that of KGM-*g*-PTMAAC implied that the graft copolymer had a spike-like surface. This was due to the introduction of the quaternary ammonium salt groups on the main

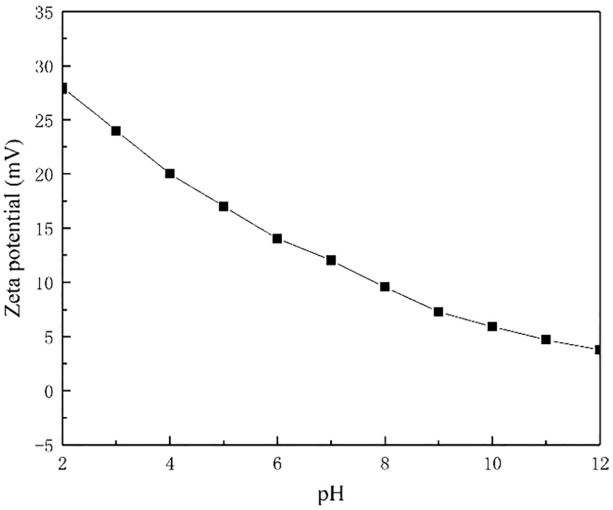

Fig. 7 pH dependence of zeta potential of the KGM-*g*-PTMAAC solution

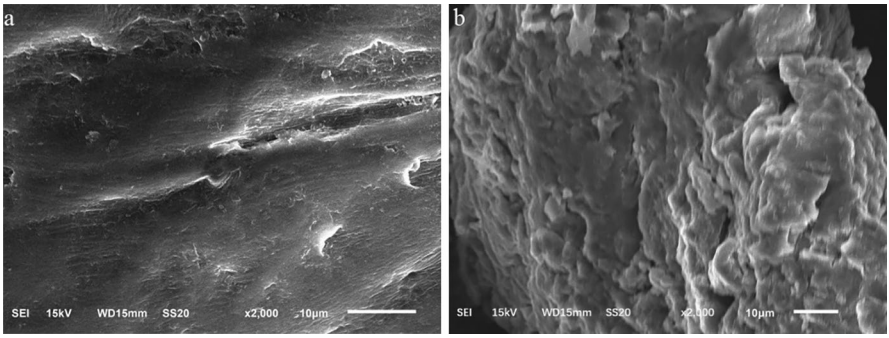

Fig. 8 SEM images of KGM (**a**) and KGM-*g*-PTMAAC (**b**)

chain of KGM resulted in significant change of the surface morphology, which further proved that TMAAC was successfully grafted onto KGM.

TG curves of samples

Figure 9 shows TG (A) and DTG (B) curves of KGM (a) and KGM-*g*-PTMAAC (b). As it is shown from TG curves, in a relatively low temperature (for example, under 320 °C), the stability of KGM-*g*-PTMAAC was poorer than that of KGM. However, in a relatively high temperature (for example, more than 320 °C), the stability of KGM-*g*-PTMAAC was better than that of KGM. And these phenomena could also be found from DTG curves. Namely, the first DTG peak of KGM-g-PTMAAC appeared in relatively lower temperature than that of KGM while the second DTG peak shifted (weak) to higher temperature than that of KGM (strong). This can

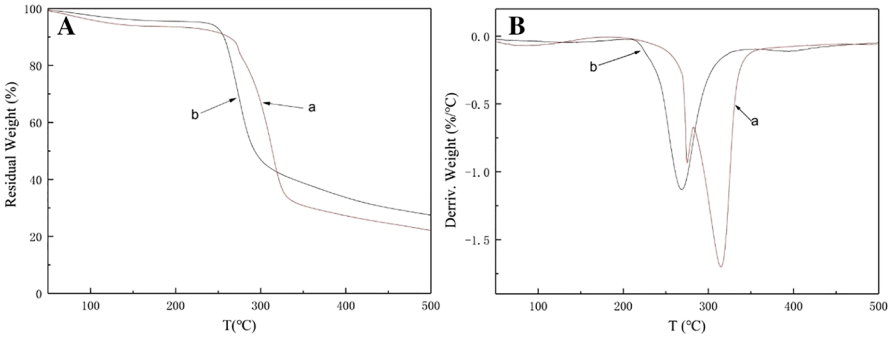

Fig. 9 TG (**A**) and DTG (**B**) curves of KGM (a) and KGM-*g*-PTMAAC (b)

probably be explained as follows: On the one hand, as the quaternary ammonium salt groups introduced onto the KGM probably undergo decomposition at a lower temperature, resulting in a lower stability of the graft copolymer. On the other hand, according to the report [45, 46], the decomposition mechanism of polysaccharides was generally involved in the dehydration reaction between molecules and the formation of polynuclear aromatic and graphitic carbon structure at high temperature. And since hydroxyl on KGM molecules was replaced by graft monomers, which prevented the elimination reaction to some extent, the thermal stability of the graft copolymer was better than that of KGM at high temperature.

Flocculation

Effect of flocculant dosage on turbidity removal rate

Figure 10 shows the influence of flocculant dosage on the turbidity removal rate. As shown in Fig. 10, when the dosage was lower than 4 mg/L, the turbidity removal rate increased with the increase in the dosage; however, when the dosage was higher than 4 mg/L, the turbidity removal rate decreased with the increase in the flocculant dosage. The coagulation–flocculation mechanism of most cationic flocculants can be explained by the synergistic effect of charge neutralization and bridging mechanism [47].

On the one hand, as it is known, the surface of kaolin particles showed negative zeta potentials in the solution [9, 25]. On the other hand, as it was mentioned above (Fig. 7), the flocculant solution presented positive zeta potentials in a wide pH range from 2.0 to 12.0. This meant that when cationic flocculant was added to kaolin suspension, the flocculants with positive charge were adsorbed on the kaolin flakes and neutralized the negative charge on their surfaces, causing the destabilization of kaolin particles and the efficient flocculation of suspensions. However, the overdosing of flocculant might lead to charge reversal and the re-stabilization of kaolin particles, which exhibited inefficient flocculation of suspensions.

On the other hand, flocculant polymers adsorbed on kaolin particles still had other free active sites for adsorbing more kaolin particles. Therefore, a so-called

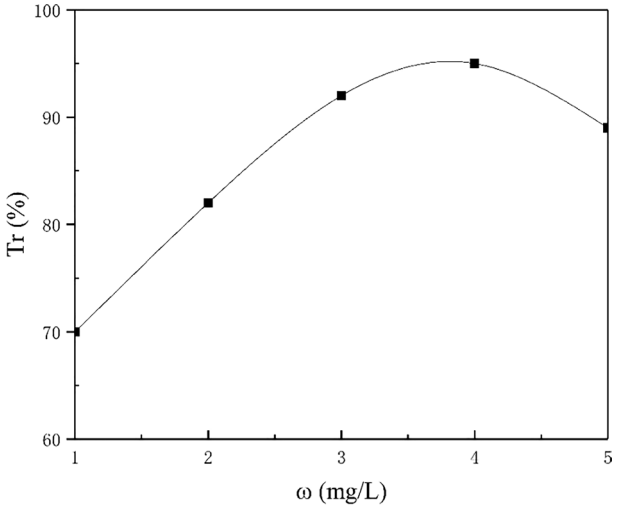

Fig. 10 Effect of flocculant dosage on turbidity removal rate

bridging effect was formed in the three-dimensional space, and the coagulation of kaolin particles occurred due to the function of gravity. When the dosage was low, the bridging effect was not obvious, and the settlement of suspended particles was not evident, i.e., Tr was relatively low. However, when the dosage of flocculant was high enough, the charge reversal occurred, thus re-stabilizing the suspended particles. Namely, the charge neutralization effect restrained the bridge effect. In addition, due to the steric hindrance of the macromolecules, the aggregation between suspended particles became difficult, which also led to the decline of Tr. Then, the best flocculant dosage was 4 mg/L in this system. However, it should be noted that although graft copolymers are likely to show self-caused turbidity in the solution, our experiments determined that the turbidity was very low (all below 1 NTU) within the whole concentration range we measured, which was similar to the findings of other searchers [20, 48]. This could be explained by the fact that both KGM and its graft copolymers had high water-solubility, leading to the low self-caused turbidity of the graft copolymers in relatively low concentration solution. Therefore, the influence of the self-caused turbidity of the flocculants on the value of Tr was not considered in this study.

Effect of pH of kaolin suspension on the turbidity removal rate

Figure 11 shows the influence of pH of kaolin suspension on the turbidity removal rate. It can be seen from Fig. 11 that, when pH value was lower than 5, the turbidity removal rate increased with the increased pH. However, when pH was higher than 5, Tr decreased as pH increasing. For cationic flocculants, their flocculation performance is evidently affected by the strength and availability of positive charges, which is relied on the cationicity and the conformation of flocculants in the aqueous solution. Of course, the pH in the solution can influence the cationicity and the

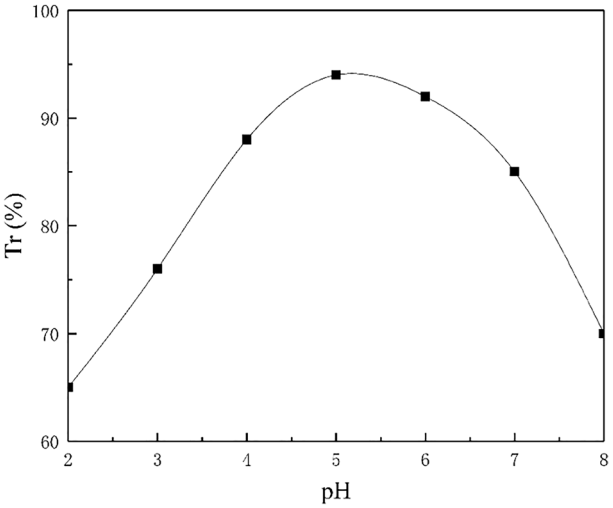

Fig. 11 Effect of pH of kaolin suspension on the turbidity removal rate

conformation of flocculants in the solution. This theory has been supported by some studies [47, 49]. Under lower pH, a large number of cations in the system resulted in the declining flexibility of polymer chains, which could not freely adjust to the appropriate conformation to form bridging effect, leading to a declined turbidity removal rate. However, under alkaline environment, both the charge neutralization and bridging effect were reduced due to the shielding effect of anionic ions on the cationic flocculants, which also reduced the turbidity removal rate. In addition, as shown in Fig. 7, the lower pH was, the higher zeta potential of a cationic flocculant solution was, which implied stronger charge neutralization with kaolin particles. This explained why the optimal pH value appeared in acidic environments (around 5 of pH).

Effect of settling time on the turbidity removal rate

Figure 12 shows the influence of flocculation time on the turbidity removal rate in the case of KGM-*g*-PTMAAC added to 1.0 wt% of kaolin suspension. The amount of KGM-*g*-PTMAAC used was 4 mg/L; the pH was 5. As it is shown in Fig. 12, when the settling time is shorter than 20 min, the turbidity removal rate of KGM-*g*-PTMAAC frequently increased with the increase in settling time. When the settling time ranged from 20 to 50 min, the turbidity removal rate increased slowly with settling time. The turbidity removal rate decreased with the settling time longer than 50 min. At the beginning, flocculants and colloidal particles could not fully contact, which was not conductive to the capture of colloidal particles by the flocculants, and the efficiency of flocculants could not be fully realized. However, after a long time of flocculation, due to the instability of bridging action, the adsorbed colloidal particles were re-dispersed into the solution, resulting in a decrease in the turbidity removal rate.

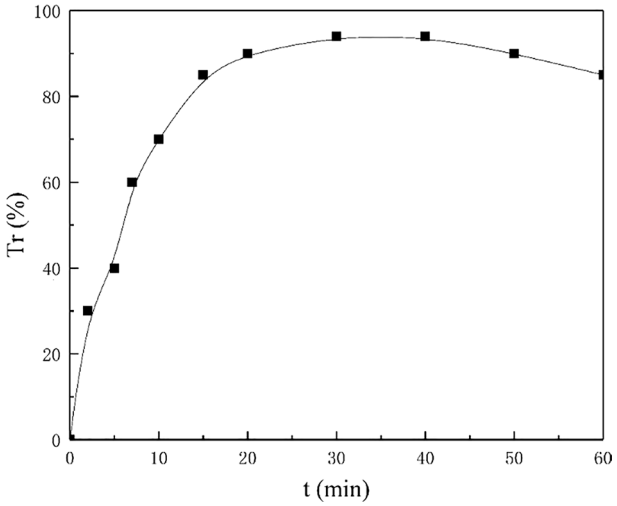

Fig. 12 Effect of settling time (*t*) on the turbidity removal rate

Effect of temperature on the turbidity removal rate

Figure 13 shows the influence of temperature on flocculation. It could be seen that, as the temperature increased, the turbidity removal rate increased at first and then decreased. When the temperature was 35 °C, the turbidity removal rate reached a maximum value. This can probably be explained as follows: When the temperature was low, the Brownian motion of colloidal particles in water was relatively slow, and the probability of collision between colloidal particles and flocculant molecules was relatively low, which did not favor the formation of flocks, and the turbidity removal rate was low. As the temperature increased, the Brownian motion of the colloidal particles was accelerated, and it could easily collide with the flocculant agents to form flocs, then the turbidity removal rate increased. However, when the temperature was too high, the rapid Brownian motion of the colloidal particles led to relatively small flocs, and the settlement of flocs was not easy to occur. Furthermore, high temperature probably also accelerated the decomposition of flocs, which was not conducive to the bridging effect, resulting in the decline of Tr.

Biodegradation properties of flocculants

Although polysaccharides have complete biodegradability, their properties cannot meet the requirements of practical application. Therefore, chemical modification must be carried out to improve their performance for practical applications. However, the premise of modification is that it does not essentially affect their degradation performance. In this work, graft modification of KGM was carried out to endow it with good flocculating properties. Figure 14 shows the biodegradation ratio of flocculants in the soil extract at different time intervals. For KGM, the degradation

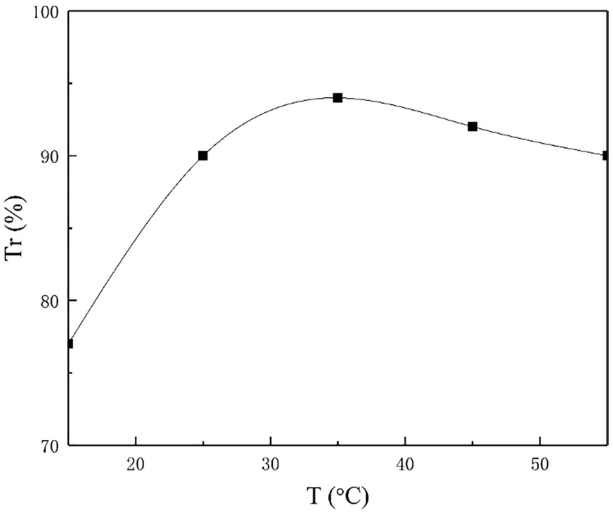

Fig. 13 Effect of temperature on the turbidity removal rate

rate was fast, which could be completely degraded in about 20 d. However, for the graft copolymer, the degradation rate was relatively slow. As shown in Fig. 14, the biodegradation ratio of flocculants achieved more than 40% within 5d and then exceeded 50% after 20 d. Subsequently, the biodegradation ratio gradually increased and attained approximately 80% after 90 d.

This probably was explained as follows: KGM was an easily biodegradable polysaccharide, while the graft copolymer contained some synthesized graft chains besides KGM as a matrix. In other words, KGM-*g*-PTMAAC had a comb-like

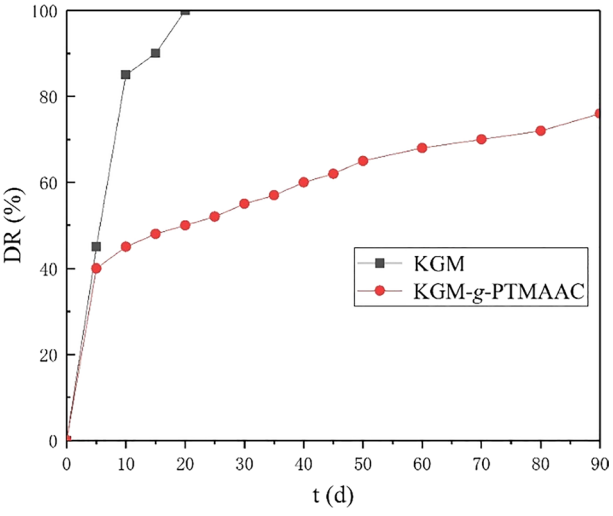

Fig. 14 Biodegradation properties of flocculants (Square, KGM; circle, KGM-*g*-PTMAAC)

structure where PTMAAC was dangled from the backbone of KGM. The secretions of the microbes from soil extracts were involved in the degradation of polysaccharides, resulting in the cleavage of chemical bonds. For KGM-*g*-PTMAAC, the degradation process started with the polymer backbone. At the beginning, there were many polysaccharides in the sample, and the microbial activity in the degradation solution was high, so the degradation rate was fast at the initial stage. However, as the polysaccharides of KGM degraded gradually, the grafted chains of PTMAAC were released. As mentioned above, KGM-*g*-PTMAAC had a comb-like structure where PTMAAC was dangled from the backbone of KGM. Obviously, microbes could split PTMAAC from the backbone of polysaccharide. Due to the slow degradation of releasing grafted chains in microorganism, the degradation ratio was no longer evidently increased when the degradation time exceeded 60 d. Therefore, in this sense, the graft copolymer could be considered as partially biodegradable, which might be mainly attributed to the grafted chains of PTMAAC. Trippathy et al. [34] in the report on the amylopectin grafted poly(acrylamide-co-*N*-methylacryamide) obtained similar results.

Conclusions

In this work, we systematically studied the preparation process, characterization and related properties of cationic flocculants based on biodegradable KGM. The graft copolymer (KGM-*g*-PTMAAC) of TMAAC with KGM was prepared using KGM as graft matrix, TMAAC as cationic monomer and CAN as initiator, respectively. The results showed that when the reaction time was 4 h, the weight ratio of TMAAC to KGM was 5:1, the amount of initiator was 0.7%, and the reaction temperature was 70 °C; the grafting yield of the product was the highest. And the interaction between the process parameters was clarified by the orthogonal experiments. Both FTIR and NMR confirmed the incorporation of quaternary ammonium cationic groups on the backbone of KGM. The SEM image showed that the morphology of the modified product was evidently different from that of unmodified KGM. The result of TG indicated that the thermal stability of KGM-*g*-PTMAAC was lower than that of KGM at relatively low temperatures, while the opposite was true at relatively high temperature. The biodegradable studied showed that the graft copolymer was partially biodegradable. Moreover, the flocculation performance test demonstrated that modified products had good flocculation for on kaolin suspension. When the dosage of KGM-*g*-PTMAAC was 4 mg/L, the pH of the medium was 5, and settling time was 30 min; the flocculation performance was the best. The obtained graft copolymer might potentially be used as a novel biodegradable flocculant in wastewater treatment.

Acknowledgements The authors are grate for the financial support from the National Natural Science Foundation of China (No: 51263009) and the Project of Team Research for Excellent Mid-Aged and Young Teachers of Higher Education of Hubei Province (No: T201006). We thank Dr. Z. W. Yu and Dr. X. Y. Han for NMR measurements.

References

1. Salgot M, Folch M (2018) Wastewater treatment and water reuse. Curr Opin Environ Sci Health 2:64–74
2. Teh CY, Budiman PM, Shak KPY, Wu TY (2016) Recent advancement of coagulation–flocculation and its application in wastewater treatment. Ind Eng Chem Res 55(16):4363–4389
3. Zhan Y, Wei R, Zhou H (2018) Improvement on the treatment of thick oil sewage by using integrated biochemical treatment technology. Int J Environ Sci Technol 15(1):81–92
4. Wang M, Payne KA, Tong S, Ergas SJ (2018) Hybrid algal photosynthesis and ion exchange (HAPIX) process for high ammonium strength wastewater treatment. Water Res 142:65–74
5. Burakov AE, Galunin EV, Burakova IV et al (2018) Adsorption of heavy metals on conventional and nanostructured materials for wastewater treatment purposes: a review. Ecotoxicol Environ Saf 148:702–712
6. Peng S, He X, Pan H (2018) Spectroscopic study on transformations of dissolved organic matter in coal-to-liquids wastewater under integrated chemical oxidation and biological treatment process. J Environ Sci 70:206–216
7. Rossi R, Yang W, Zikmund E, Pant D, Logan BE (2018) In situ biofilm removal from air cathodes in microbial fuel cells treating domestic wastewater. Bioresour Technol 265:200–206
8. Pal S, Mal D, Singh RP (2005) Cationic starch: an effective flocculating agent. Carbohydr Polym 59(4):417–423
9. Zhu H, Zhang Y, Yang X et al (2015) One-step green synthesis of non-hazardous dicarboxyl cellulose flocculant and its flocculation activity evaluation. J Hazard Mater 296:1–8
10. Renault F, Sancey B, Badot PM, Crini G (2009) Chitosan for coagulation/flocculation processes—an eco-friendly approach. Eur Polym J 45(5):1337–1348
11. Banerjee C, Ghosh S, Sen G, Mishra S, Shukla P, Bandopadhyay R (2013) Study of algal biomass harvesting using cationic guar gum from the natural plant source as flocculant. Carbohydr Polym 92(1):675–681
12. Dryabina S, Fotina K, Navrotskii A, Novakov I (2017) The flocculation of kaolin aqueous dispersion by two cationic polyelectrolytes. Colloids Surf A 515:12–21
13. Ma J, Shi J, Ding L et al (2018) Removal of emulsified oil from water using hydrophobic modified cationic polyacrylamide flocculants synthesized from low-pressure UV initiation. Sep Purif Technol 197:407–417
14. Kajihara M, Aoki D, Matsushita Y, Fukushima K (2018) Synthesis and characterization of lignin-based cationic dye-flocculant. J Appl Polym Sci 135(32):46611
15. El-Naggar ME, Samhan FA, Salama AAA, Hamdy RM, Ali GH (2018) Cationic starch: safe and economic harvesting flocculant for microalgal biomass and inhibiting *E. coli* growth. Int J Biol Macromol 116:1296–1303
16. Su Y, Du H, Huo Y et al (2016) Characterization of cationic starch flocculants synthesized by dry process with ball milling activating method. Int J Biol Macromol 87:34–40
17. Katsuraya K, Okuyama K, Hatanaka K, Oshima R, Sato T, Matsuzaki K (2003) Constitution of konjac glucomannan: chemical analysis and ^{13}C NMR spectroscopy. Carbohydr Polym 53(2):183–189
18. Tian D, Zhou Y, Xiong L, Lu F (2017) Synthesis and properties of caffeine molecularly imprinted polymers based on konjac glucomannan. Adv Polym Technol 36(1):68–76
19. Zhu F (2018) Modifications of konjac glucomannan for diverse applications. Food Chem 256:419–426
20. Dai S, Jiang F, Shah NP, Corke H (2017) Stability and phase behavior of konjac glucomannan-milk systems. Food Hydrocoll 73:30–40
21. Lei W, Yang Q, Jia X, Zhang T (2010) Preparation and antimicrobial activity of Konjac Glucomannan modified with quaternary ammonium compound. J Appl Polym Sci 118(6):3453–3459
22. Yu H, Huang Y, Ying H, Xiao C (2007) Preparation and characterization of a quaternary ammonium derivative of konjac glucomannan. Carbohydr Polym 69(1):29–40
23. Wang K, Gao S, Shen C et al (2018) Preparation of cationic konjac glucomannan in NaOH/urea aqueous solution. Carbohydr Polym 181:736–743
24. Tian D, Wu X, Liu C, Xie H-Q (2010) Synthesis and flocculation behavior of cationic konjac glucomannan containing quaternary ammonium substituents. J Appl Polym Sci 115(4):2368–2374
25. Ren WJ, Zhang AQ, Qin SY, Li ZK (2016) Synthesis and evaluation of a novel cationic konjac glucomannan-based flocculant. Carbohydr Polym 144:238–244
26. Garcia-Valdez O, Champagne P, Cunningham MF (2018) Graft modification of natural polysaccharides via reversible deactivation radical polymerization. Prog Polym Sci 76:151–173
27. Shi Z, Jia C, Wang D et al (2019) Synthesis and characterization of porous tree gum grafted copolymer derived from *Prunus cerasifera* gum polysaccharide. Int J Biol Macromol 133:964–970

28. Deng F, Zhang Y, Ge X, Li M, Li X, Cho UR (2016) Graft copolymers of microcrystalline cellulose as reinforcing agent for elastomers based on natural rubber. J Appl Polym Sci 133(9)
29. Li M-C, Lee JK, Cho UR (2012) Synthesis, characterization, and enzymatic degradation of starch-grafted poly(methyl methacrylate) copolymer films. J Appl Polym Sci 125(1):405–414
30. Meimoun J, Wiatz V, Saint-Loup R et al (2018) Modification of starch by graft copolymerization. Starch-Stärke 70(1–2):1600351
31. Huang M, Liu Z, Li A, Yang H (2017) Dual functionality of a graft starch flocculant: flocculation and antibacterial performance. J Environ Manag 196:63–71
32. Işıklan N, Kurşun F, Inal M (2009) Graft copolymerization of itaconic acid onto sodium alginate using ceric ammonium nitrate as initiator. J Appl Polym Sci 114(1):40–48
33. Pal S, Ghorai S, Dash MK, Ghosh S, Udayabhanu G (2011) Flocculation properties of polyacrylamide grafted carboxymethyl guar gum (CMG-g-PAM) synthesised by conventional and microwave assisted method. J Hazard Mater 192(3):1580–1588
34. Sasmal D, Singh RP, Tripathy T (2015) Synthesis and flocculation characteristics of a novel biodegradable flocculating agent amylopectin-g-poly(acrylamide-co-*N*-methylacrylamide). Colloids Surf A 482:575–584
35. Hocine T, Benhabib K, Bouras B, Mansri A (2017) Comparative study between new polyacrylamide based copolymer poly(AM-4VP) and a cationic commercial flocculant: application in turbidity removal on semi-industrial pilot. J Polym Environ 26(4):1550–1558
36. Liu Z, Lu X, Xie J, Feng B, Han Q (2019) Synthesis of a novel tunable lignin-based star copolymer and its flocculation performance in the treatment of kaolin suspension. Sep Purif Technol 210:355–363
37. Mu R-J, Yuan Y, Wang L et al (2018) Microencapsulation of *Lactobacillus acidophilus* with konjac glucomannan hydrogel. Food Hydrocoll 76:42–48
38. Phang Y-N, Chee S-Y, Lee C-O, Teh Y-L (2011) Thermal and microbial degradation of alginate-based superabsorbent polymer. Polym Degrad Stab 96(9):1653–1661
39. McDowall DJ, Gupta BS, Stannett VT (1984) Grafting of vinyl monomers to cellulose by ceric ion initiation. Prog Polym Sci 10(1):1–50
40. Pourjavadi A, Zeidabadi F, Barzegar S (2010) Alginate-based biodegradable superabsorbents as candidates for diclofenac sodium delivery systems. J Appl Polym Sci 118(4):2015–2023
41. Vieira MC, Gil AM (2005) A solid state NMR study of locust bean gum galactomannan and Konjac glucomannan gels. Carbohydr Polym 60(4):439–448
42. Crescenzi V, Dentini M, Masci G et al (2002) A high field NMR study of the products ensuing from konjak glucomannan C(6)-oxidation followed by enzymatic C(5)-epimerization. Biomacromol 3(6):1343–1352
43. Gidley MJ, McArthur AJ, Underwood DR (1991) ^{13}C NMR characterization of molecular structures in powders, hydrates and gels of galactomannans and glucomannans. Food Hydrocoll 5(1):129–140
44. Haack V, Heinze T, Oelmeyer G, Kulicke W-M (2002) Starch derivatives of high degree of functionalization, 8. Synthesis and flocculation behavior of cationic starch polyelectrolytes. Macromol Mater Eng 287(8):495–502
45. Morita H (1956) Characterization of starch and related polysaccharides by differential thermal analysis. Anal Chem 28(1):64–67
46. Singh B, Sharma V, Pal L (2011) Formation of sterculia polysaccharide networks by gamma rays induced graft copolymerization for biomedical applications. Carbohydr Polym 86(3):1371–1380
47. Fang R, Cheng X, Xu X (2010) Synthesis of lignin-base cationic flocculant and its application in removing anionic azo-dyes from simulated wastewater. Bioresour Technol 101(19):7323–7329
48. Bokias G, Mylonas Y, Staikos G, Bumbu GG, Vasile C (2001) Synthesis and aqueous solution properties of novel thermoresponsive graft copolymers based on a carboxymethylcellulose backbone. Macromolecules 34(14):4958–4964
49. Somasundaran P, Runkana V (2005) Investigation of the flocculation of colloidal suspensions by controlling adsorbed layer microstructure and population balance modelling. Chem Eng Res Des 83(7):905–914